AGU PUBLICATIONS

Geophysical Research Letters

RESEARCH LETTER
10.1002/2016GL070078

Key Points:
- Volcanic monitoring with seismic noise cross-correlation techniques can be achieved with a single three-component seismic station
- The single station cross component approach provides more stable results than autocorrelation
- Environmental perturbations have a different signature from volcanic perturbations and can therefore be discriminated

Supporting Information:
- Supporting Information S1
- Figure S2
- Figure S3

Correspondence to:
R. S. M. De Plaen,
raphael.deplaen@uni.lu

Citation:
De Plaen, R. S. M., T. Lecocq, C. Caudron, V. Ferrazzini, and O. Francis (2016), Single-station monitoring of volcanoes using seismic ambient noise, *Geophys. Res. Lett.*, *43*, 8511–8518, doi:10.1002/2016GL070078.

Received 17 JUN 2016
Accepted 9 AUG 2016
Accepted article online 11 AUG 2016
Published online 30 AUG 2016

©2016. American Geophysical Union. All Rights Reserved.

Single-station monitoring of volcanoes using seismic ambient noise

Raphael S. M. De Plaen[1], Thomas Lecocq[2], Corentin Caudron[3], Valérie Ferrazzini[4], and Olivier Francis[1]

[1]Faculté des Sciences, de la Technologie et de la Communication, University of Luxembourg, Luxembourg, Luxembourg, [2]Royal Observatory of Belgium, Uccle, Belgium, [3]Department of Earth Sciences, University of Cambridge, Cambridge, UK, [4]Observatoire Volcanologique du Piton de la Fournaise, Institut de Physique du Globe de Paris, Sorbonne Paris Cité, Paris VII - Denis Diderot University, CNRS, Réunion, France

Abstract Seismic ambient noise cross correlation is increasingly used to monitor volcanic activity. However, this method is usually limited to volcanoes equipped with large and dense networks of broadband stations. The single-station approach may provide a powerful and reliable alternative to the classical "cross-station" approach when measuring variation of seismic velocities. We implemented it on the Piton de la Fournaise in Reunion Island, a very active volcano with a remarkable multidisciplinary continuous monitoring. Over the past decade, this volcano has been increasingly studied using the traditional cross-correlation technique and therefore represents a unique laboratory to validate our approach. Our results, tested on stations located up to 3.5 km from the eruptive site, performed as well as the classical approach to detect the volcanic eruption in the 1–2 Hz frequency band. This opens new perspectives to successfully forecast volcanic activity at volcanoes equipped with a single three-component seismometer.

1. Introduction

Volcanoes are studied and monitored using diverse instrument networks. Data recorded by the instruments are generally turned into proxies to assess the state of the volcano. The ultimate goal of volcano observatories is to identify changes in a volcanic edifice as far ahead in time of an eruption as possible. The efficiency of this monitoring is critically related to the detection and understanding of slight changes in the edifice long before the start of the magma transport during active volcanic episodes. During volcanic eruptions, magma transport causes gas release, pressure perturbations in the plumbing system [*Patane*, 2006], and potential surface deformation that can be detected using geodetic techniques [e.g., *Peltier et al.*, 2009, 2016; *Staudacher et al.*, 2009]. However, the sensitivity of these techniques to deep changes can be limited [e.g., *Chaussard et al.*, 2013], leaving room for a better early warning solution.

Alternatively, deep mechanical processes associated with magma pressurization and/or migration and their spatial-temporal evolution can be monitored with volcanic seismicity and yield precise locations and mechanisms for earthquakes and volcanic tremor [e.g., *Battaglia et al.*, 2005; *Massin et al.*, 2011; *Lengliné et al.*, 2016]. Yet seismicity only provides information on short-term phenomenon (few seconds to few days) and is inadequate to expose early aseismic processes such as magma pressurization [*Brenguier et al.*, 2008b].

Seismic interferometry uses the multiple scattering of seismic vibrations by heterogeneities in the crust. Implemented on coda waves of earthquakes or seismic ambient noise, this technique allows to retrieve the Green's function for surface waves between two stations by cross correlating these diffuse wavefields [e.g., *Lobkis and Weaver*, 2001; *Derode et al.*, 2003; *Snieder*, 2004; *Wapenaar*, 2004]). This technique is increasingly used as a nondestructive way to continuously monitor small seismic velocity changes (~0.1%) associated with variations of heat, pressure, or water saturation in the subsurface [*Grêt et al.*, 2006; *Sens-Schönfelder and Wegler*, 2006]. Seismic velocity changes are typically measured from the cross-correlation functions (CCF) for each pair of stations and eventually averaged over the whole network to yield more stable results. The cross-correlation (CC) technique has been extensively described over the past decade, with many available reviews [e.g., *Larose et al.*, 2006; *Bensen et al.*, 2007; *Wapenaar et al.*, 2010a, 2010b; *Sens-Schönfelder and Wegler*, 2011]. Seismic velocity variation measurements using the CC technique are used for monitoring [*Snieder and Hagerty*, 2004; *Brenguier et al.*, 2008b; *Hadziioannou et al.*, 2011] with applications for volcanoes [e.g., *Sens-Schönfelder and Wegler*, 2006; *Duputel et al.*, 2009; *Mordret et al.*, 2010; *Caudron et al.*, 2015], large magnitude earthquakes in the far field [*Wegler and Sens-Schönfelder*, 2007; *Brenguier et al.*, 2008a; *Ohmi*

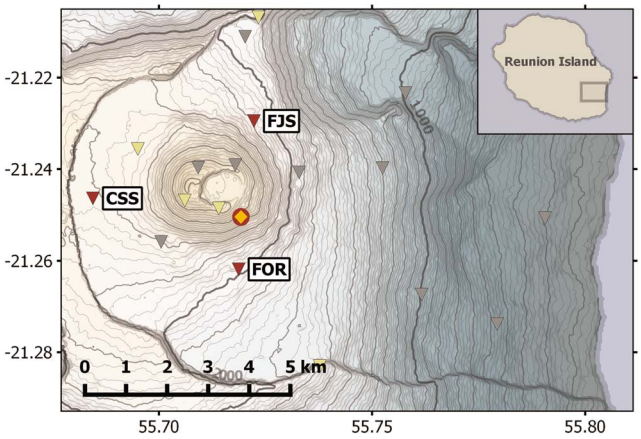

Figure 1. Map of the stations used for this study (red triangles) and the OVPF seismic network (triangles). The yellow triangles represent short-period seismometers, the remaining are broadband seismometers. Station FOR is closer to the 2014 fissure eruption (circle).

et al., 2008; *Wegler et al*., 2009; *Hobiger et al*., 2012; *Minato et al*., 2012], and smaller magnitude earthquakes at smaller distances [*Maeda et al*., 2010; *D'Hour et al*., 2015]. In most cases, relative velocity changes have been evidenced using a large number of stations and of station pairs. The technique is also applicable to single stations, using one (or all) component of a one-component (or three-component) seismometers. The single-station approach has been successfully applied to study earthquakes [*Sens-Schönfelder and Wegler*, 2006; *Wegler and Sens-Schönfelder*, 2007; *Hobiger et al*., 2014; *Nakahara*, 2014; *D'Hour et al*., 2015].

In this study, we apply this approach to volcano monitoring using a small network. In addition, we explore the possibility to exploit higher frequencies than traditional ambient noise monitoring approaches and eventually open the path to systematically make use of short-period seismometers for seismic velocity monitoring on volcanoes. We focus on the Piton de la Fournaise (PdF), a basaltic shield volcano located in the ESE part of Reunion Island (France) in the Indian Ocean. It is one of the world's most active volcanoes with, on average, one eruption every year. The PdF is extensively monitored with a broad range of instruments, and many studies use the seismic noise cross-correlation method with multiple stations to measure seismic velocity changes associated to its activity [*Brenguier et al*., 2008b, 2011; *Duputel et al*., 2009; *Clarke et al*., 2013; *Rivet et al*., 2014, 2015; *Sens-Schönfelder et al*., 2014]. We studied data acquired by three seismic stations in 2014, containing one eruption in June and several environmental perturbations recorded throughout the year. This background provides a consistent base of comparison to test the robustness of the single-station approach.

2. Data and Method

2.1. Data

We used seismic data from the Piton de la Fournaise Volcano Observatory Network (OVPF, Institut de Physique du Globe de Paris), Reunion island, acquired in 2014 (Figure 1). At that time, the monitoring network of the PdF was composed of 25 continuously recording stations, i.e. 8 short period and 17 broadband. This data set covers a 1 day eruption on 21 June 2014 that followed 4 years of quiescence. We focused our analysis on broadband stations CSS, FJS, and FOR, which are at similar distances from the crater Dolomieu, the main crater of the PdF. Among them, station FOR is the closest to the 2014 fissure eruption (Figure 1). In parallel, we analyzed a catalogue of earthquakes located manually along with the rainfall measured at a meteorological station next to station FOR.

2.2. Method

Seismic velocity changes are measured from seismic noise cross correlation following a workflow similar to *Lecocq et al*. [2014]: Seismic records for all components are preprocessed by carefully checking for their timing (sample alignment), gaps (interpolating or tapering between gaps), then bandpass prefiltered between 0.01 and 8.0 Hz and resampled to 20 Hz prior to whitening and cross correlation.

Traditionally, ambient seismic noise is cross correlated between pairs of stations. This approach was adopted in an earlier study by *Rivet et al*. [2015] and is compared with our results in section 3.4. In contrast, we performed two types of processing based on the single-station approach: Single-station cross component (SC) and each component with itself or autocorrelation (AC). The spectral whitening that sets the amplitude of the signal to 1 for all frequencies was not applied for AC since only the phase of the signal would remain and the autocorrelation of such a signal does not contain information on the medium anymore. For both

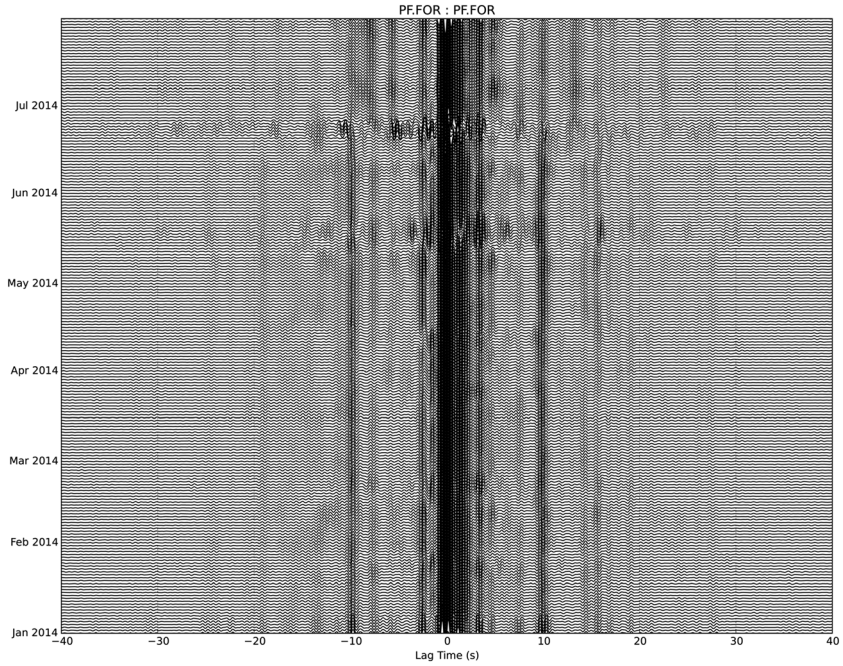

Figure 2. Plot of the cross-correlation functions (CCF) with time for station FOR, components pair *ZE* and 5 day stack. The data were filtered between 1 and 2 Hz and clipped in the time domain at 3 times the standard deviation. Stable phases can clearly be identified up to about 30 s of lag time.

AC and SC the data were then filtered in different frequency ranges (0.01–1.0 Hz, 0.5–1.0 Hz, 1.0–2.0 Hz, and 2.0–4.0 Hz) and the performance of 1-bit normalization as well as clipping at 3 times the RMS of each time window was tested as time domain normalization. Clipping eventually provided the most stable results and was therefore chosen for this study.

The cross correlation and autocorrelation were then computed for each individual day, between all the possible combinations of components (three SC and three AC for each station) and for all the different filters, before being averaged with a 5 day linear stacking to maximize the signal-to-noise ratio (Figure 2).

The plot of CCFs over time shows coherent phases in the late part of the coda for different days (e.g., +10 s time lag). Shifts in time from these coherent phases, even if not visible on Figure 2, are interpreted as changes of seismic velocity in the crust that can be measured. With the assumption of a homogeneous change in the medium, we considered that the relative differences in travel time dt are due to the change in the seismic velocity dv as $-\mathrm{d}t/t = \mathrm{d}v/v$ [*Ratdomopurbo and Poupinet*, 1995].

Temporal velocity variations in the medium are measured on both the negative and the positive sides of the CCF, for time lags between 5 and 35 s, preventing direct wave contamination. Each individual CCF (daily) is compared to a reference CCF that averages the results for the whole period of study. The travel time changes are measured in the frequency domain using the Multiple-Window Cross-Spectral Analysis method with a quality control using coherency and the error of the linear regression in the time domain [*Poupinet et al.*, 1984; *Brenguier et al.*, 2011]. The velocity variations calculated with the SC and the AC are then ultimately averaged by station for each frequency band.

3. Results and Discussion

3.1. Frequency Dependence

Comparing dv/v curves for station FOR in Figure 3 shows that the SC (a) is significantly more stable than the AC (b) at the lowest frequencies. The AC exhibits a very strong variability with a higher signal-to-noise ratio starting from the 0.5–1.0 Hz frequency band. The SC already shows a distinct preeruptive seismic velocity drop in the 0.1–1.0 frequency band (Figure 3a). In the 1.0–2.0 Hz frequency band the SC (Figure 3e) is sensitive to both heavy rainfall events and the volcanic eruption (blue and red vertical lines, respectively) with a larger

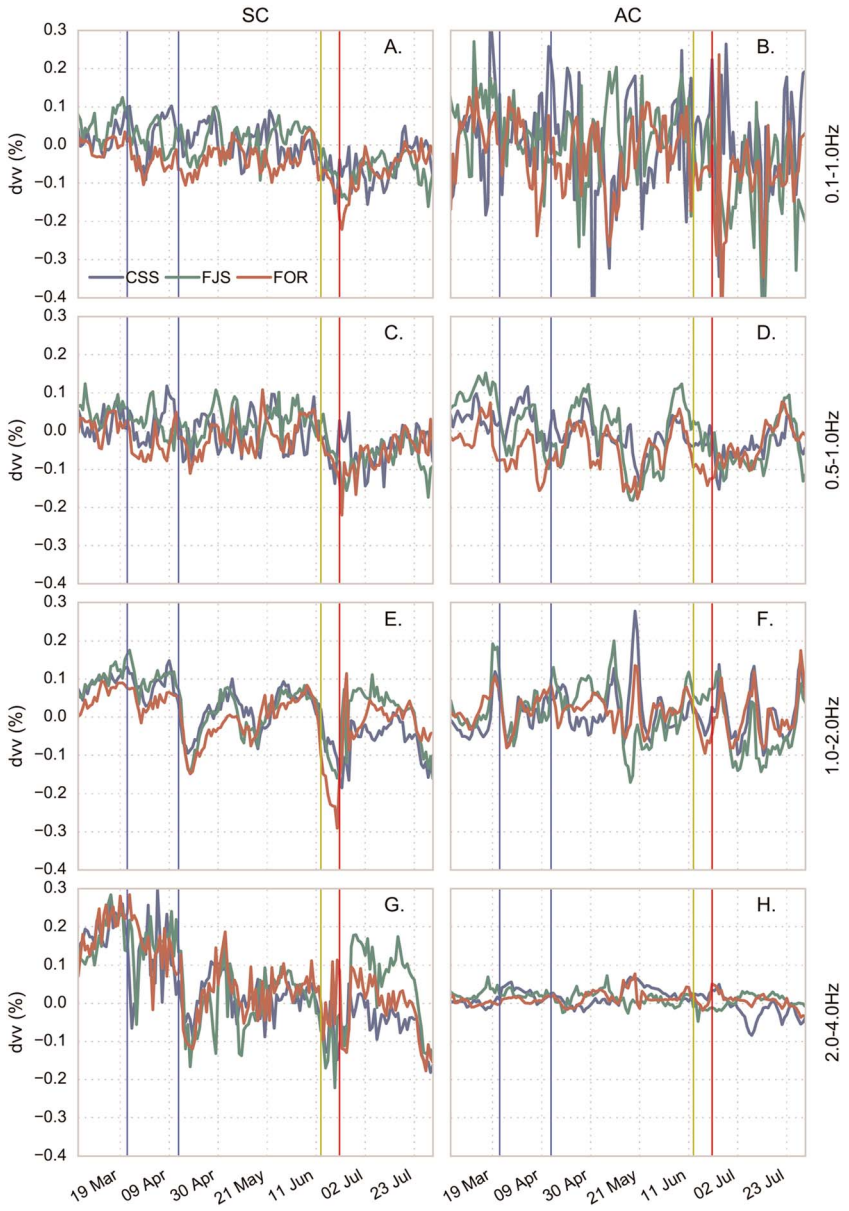

Figure 3. Variation of seismic velocity for three stations (CSS, FJS, and FOR) and four frequency ranges (from top to bottom, (a, b) 0.1–1.0 Hz, (c, d) 0.5–1.0 Hz, (e, f) 1.0–2.0 Hz, and (g, h) 2.0–4.0 Hz) measured using single-station cross components (SC; Figures 3a, 3c, 3e, and 3g) and autocorrelation (AC; Figures 3b, 3d, 3f, and 3h). The vertical lines represent high rainfalls (blue), increasing seismicity (yellow), and the eruption day (red). The 95% confidence limits are shown in Figure S2.

drop before the eruption (~0.3%, station FOR) than for the rainfall (~0.15%, station FOR). The AC (Figure 3f) is also sensitive to rainfall and the volcanic eruption in that frequency band. However, a larger-amplitude perturbation affects the observation between 10 and 20 May and in early July. This perturbation is consistent for all three stations and seems to have little effect on the SC processing. No rainfall or seismic activity (blue and yellow vertical lines, respectively) seems to correspond to this seismic velocity change. The contamination of the AC by high-amplitude events such as earthquakes is a known issue since no spectral whitening can be used to mitigate them. Here the perturbation was probably caused by storms and very strong winds which were recorded those days [*Meteo-France Direction Interrégionale Océan Indien*, 2014] and are known to affect high frequencies [*Withers et al.*, 1996]. Differences between AC and SC are again more pronounced in the 2.0–4.0 Hz frequency band with an increased variability for the SC (Figure 3g) opposed to the AC (Figure 3 h), which exhibits less variability but also a smaller signal-to-noise ratio.

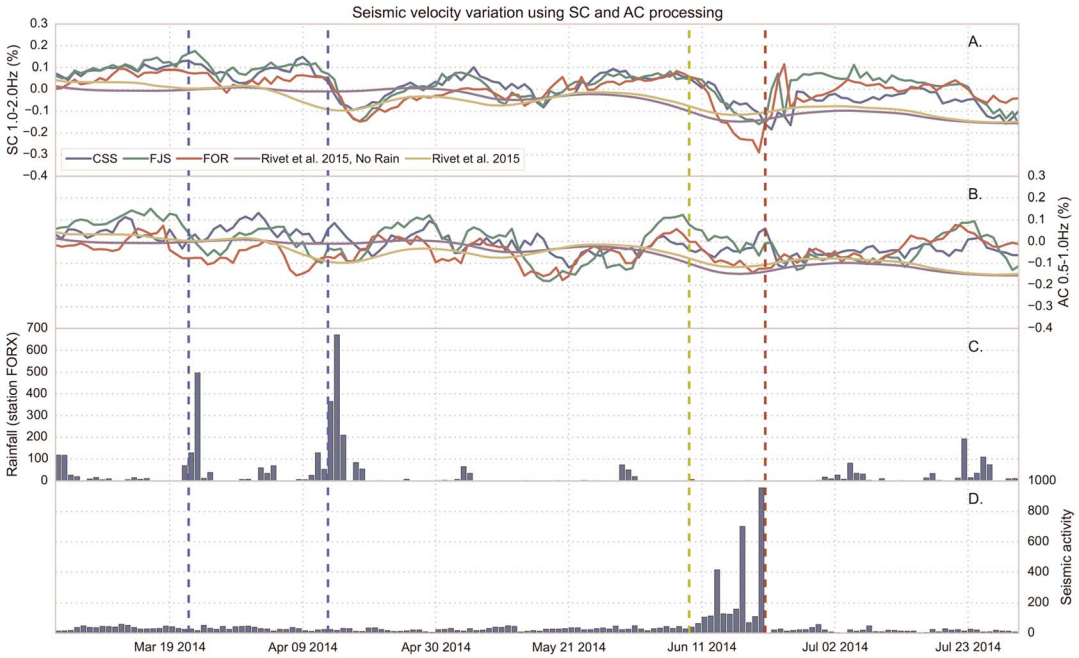

Figure 4. Seismic velocity variations calculated using (a) single-station cross components (SC, 1.0–2.0 Hz) and (b) autocorrelation (AC, 0.5–1.0 Hz) at Piton de la Fournaise volcano (5 days stacking) along with (c) the rainfall and (d) the seismic activity between March and July 2014. The vertical lines represent high rainfalls, increasing seismicity and the day of the eruption in blue, yellow, and red, respectively. Results digitized from *Rivet et al.* [2015] are shown for comparison.

The SC clearly provides better results than AC in terms of stability and clarity for the preeruptive decrease of seismic velocity. For all three stations, the preeruptive velocity drop is clearly detected. The best results are obtained in the 0.5–1 Hz and the 1–2 Hz frequency bands (Figures 3c and 3e), with the highest signal to noise ratio being reached in the 1–2 Hz frequency band. The best performance at these frequency bands could be caused by a higher power at these frequencies of the ambient noise field (Figure S3 in the supporting information).

3.2. Seismicity

Figure 4 shows our results (a and b) along with the rainfall (c) and the seismic activity (d). SC (Figure 4a) and AC (Figure 4b) the 1.0–2.0 Hz and 0.5–1.0 Hz frequency bands respectfully show the best signal-to-noise ratio and sensitivity to the noteworthy events that occurred during the studied period. Considerable rainfall (blue vertical lines, the value exceeds 3 times the RMS) caused a drop in seismic velocity of similar magnitude at all three stations which are always observed, except in April with the AC approach. Another drop precedes the 21 June eruption (red vertical line) and could indicate a preeruptive decrease in seismic velocity.

Before 9 June, the seismicity remained at a very low level with less than 30 earthquakes per day, a vast majority of which were identified as rockfalls. On 11 June the drop in seismic velocity seems to have begun independently from the number of earthquakes (less than five per hour) and their magnitudes. The seismicity eventually increased due to summit activity and as the seismic velocity dropped it finally reached a peak the day before the eruption (955 earthquakes; 846 from summit activity). After the eruption, the seismicity became very low, dominated by rockfalls again (Figures 4 and S1).

A large number of volcano-tectonic earthquakes at PdF volcano were relocated by *Lengliné et al.* [2016] for 2014 and 2015. They identified a persistent shallow (~700 m above sea level) preeruptive ring-shaped cluster under the summit crater associated with a westward migration of its southern part before the eruption. They interpreted the repetitive occurrence of earthquakes along this structure as possible preexisting zones of weakness within the edifice that are triggered by static stress changes linked to an overpressurization of the magma chamber or dike intrusions in the volcanic edifice. The same process likely caused the preeruptive seismic velocity drop, which was therefore concomitant to the increase of seismic activity. Although we interpreted the preeruptive velocity drop as a result of the buildup of pressure in the

subsurface, we cannot completely preclude an influence of the simultaneous increase of seismic activity or migration of earthquakes.

The seismicity could ultimately contaminate our observation in the microseismic frequency band but only affecting direct waves when we are looking further in the coda. It could also be assumed that high seismicity is required to perform good observations of seismic velocity variation with this technique. However, lower seismicity did not prevent us from observing rainfall-associated velocity drops (blue vertical lines; Figure 4), ruling out this assumption.

3.3. Station by Station Comparison

The station geographically closest to the fissure eruption (FOR) clearly displays a significantly larger drop (~0.3%) than the two others (<0.1%) for both processing approaches. By contrast, the three stations display the same amplitude for the rainfall-associated drop (0.05–0.1%). We interpreted this as a larger-scale distribution of rainfall which, unlike the volcanic eruption, affects the three stations in the same way. This noteworthy difference could provide a way to discriminate the causes of seismic velocity change when the single-station approach is used.

3.4. Comparison With Rivet et al. [2015]

Rivet et al. [2015] studied the temporal variation of seismic velocity using seismic noise correlation in the traditional CC approach with all the 27 stations of the OVPF network. They used only vertical components bandpass filtered between 0.25 and 2 Hz combined with 1 bit normalization, 8 days stacking, "long-term variation removal"(sic.), and network-wide averaging to observe the preeruptive drop of seismic velocity. They extended their observation to the preceding low-activity period and highlighted seismic velocity variations highly correlated with rainfall episodes and subsequent pore pressure perturbation.

Figure 4 shows the results from *Rivet et al*. [2015], before and after they were corrected for the rainfall effect, along with our results for SC and AC processing. Their results unsurprisingly do not seem to exhibit the same temporal resolution as our results because they averaged the pairs from all the network stations, used 8 days stacking and possibly also some extra fitting/sliding mean [*Brenguier et al*., 2008b; *Clarke et al*., 2013].

There is a striking correlation between their results obtained with the CC and all the pairs from the 27 stations network and our results obtained with one station at a distance up to 3.6 km from the eruptive vent. The single-station approach clearly appears as a promising alternative when the CC cannot be efficiently implemented. These unfavorable scenarios include volcanoes equipped with only one or too few seismic stations as well as analysis where the CC provides across-correlation coefficient between the CCFs and the reference that is too low. Additionally, short-period instruments are not always used for cross-correlation analysis due to strong attenuation of high frequencies between far apart station pairs that affect the measurement of seismic velocity variations. The frequency bands used in our analysis are dominated by microseismic energy and would therefore likely work everywhere for seismic velocity monitoring, including with short-period instruments.

4. Conclusions

Like the traditional cross-correlation approach implemented by *Rivet et al*. [2015], both the single-station cross component (SC) and the autocorrelation (AC) approaches successfully detected the preeruptive seismic velocity drop along with other extreme climatic perturbations in 2014. The good performance of the single-station approaches opens the possibility to use noise cross-correlation techniques on volcanoes equipped with only one of too few instruments or poorly correlated station pairs.

The AC exhibits poorer results than the SC in terms of stability, a lower preeruptive velocity drop, and a sensitivity to strong-amplitude events that the SC does not have. More work is still required to better mitigate the contamination of strong amplitude events on the AC with solutions such as using phase cross correlation over the classical cross correlation [*Schimmel*, 1999; *Schimmel and Gallart*, 2007; *Schimmel et al*., 2011; *D'Hour et al*., 2015] which will be left to a future study. The best performance for the SC and the AC are obtained in the 1–2 Hz and the 0.5–1 Hz frequency bands, respectively. The good performance at high frequencies could be associated to the higher amplitude of those frequencies in the ambient noise content that "illuminates"

the change in the medium, providing a clear, stable observation of the velocity drop. These results also show that short-period seismometers could probably be used with the single-station approach.

The volcanic eruption and the rainfall have a different effect on the seismic velocity measured at distinct stations. The rainfall has a similar impact on all the stations, while the volcanic eruption has a greater effect on the closest station. Still, it should be noted that even the most distant station (station CSS, 3.65 km from the eruptive site) clearly detected the preeruptive velocity drop using both the SC and the AC. These results open new perspective to monitor volcanoes using seismic velocity variations where the traditional cross-correlation analysis cannot be performed.

Acknowledgments

We thank Aline Peltier for her help, comments and advice. The data used in this paper were collected by the Observatoire Volcanologique du Piton de la Fournaise/Institute de Physique du Globe de Paris (OVPF/IPGP). The codes used are modified from the MSNoise python package [*Lecocq et al*., 2014]. C. Caudron was supported by a Fondation Wiener Anspach postdoctoral fellowship. We are grateful to Martha Savage and an anonymous reviewer for their helpful comments.

References

Battaglia, J., K. Aki, and T. Staudacher (2005), Location of tremor sources and estimation of lava output using tremor source amplitude on the Piton de la Fournaise volcano: 2. Estimation of lava output, *J. Volcanol. Geotherm. Res.*, *147*(3-4), 291–308, doi:10.1016/j.jvolgeores.2005.04.006.

Bensen, G. D., M. H. Ritzwoller, M. P. Barmin, A. L. Levshin, F. Lin, M. P. Moschetti, N. M. Shapiro, and Y. Yang (2007), Processing seismic ambient noise data to obtain reliable broad-band surface wave dispersion measurements, *Geophys. J. Int.*, *169*(3), 1239–1260.

Brenguier, F., M. Campillo, C. Hadziioannou, N. M. Shapiro, R. M. Nadeau, and E. Larose (2008a), Postseismic relaxation along the San Andreas fault at Parkfield from continuous seismological observations, *Science*, *321*(5895), 1478–81, doi:10.1126/science.1160943.

Brenguier, F., N. M. Shapiro, M. Campillo, V. Ferrazzini, Z. Duputel, O. Coutant, and A. Nercessian (2008b), Towards forecasting volcanic eruptions using seismic noise, *Nat. Geosci.*, *1*(2), 126–130, doi:10.1038/ngeo104.

Brenguier, F., D. Clarke, Y. Aoki, N. M. Shapiro, M. Campillo, and V. Ferrazzini (2011), Monitoring volcanoes using seismic noise correlations, *Comptes Rendus Geosci.*, *343*(8-9), 633–638, doi:10.1016/j.crte.2010.12.010.

Caudron, C., T. Lecocq, D. K. Syahbana, W. McCausland, A. Watlet, T. Camelbeeck, A. Bernard, and Surono (2015), Stress and mass changes at a "wet" volcano: Example during the 2011–2012 volcanic unrest at Kawah Ijen volcano (Indonesia), *J. Geophys. Res. Solid Earth*, *120*, 5117–5134, doi:10.1002/2014JB011590.

Chaussard, E., F. Amelung, and Y. Aoki (2013), Characterization of open and closed volcanic systems in Indonesia and Mexico using InSAR time series, *J. Geophys. Res. Solid Earth*, *118*, 3957–3969, doi:10.1002/jgrb.50288.

Clarke, D., F. Brenguier, J. L. Froger, N. M. Shapiro, A. Peltier, and T. Staudacher (2013), Timing of a large volcanic flank movement at Piton de la Fournaise Volcano using noise-based seismic monitoring and ground deformation measurements, *Geophys. J. Int.*, *195*(2), 1132–1140, doi:10.1093/gji/ggt276.

D'Hour, V., M. Schimmel, A. F. Do Nascimento, J. M. Ferreira, and H. C. Lima Neto (2015), Detection of subtle hydromechanical medium changes caused by a small-magnitude earthquake swarm in NE Brazil, *Pure Appl. Geophys.*, doi:10.1007/s00024-015-1156-0.

Derode, A., E. Larose, M. Campillo, and M. Fink (2003), How to estimate the Green's function of a heterogeneous medium between two passive sensors?, Application to acoustic waves, *Appl. Phys. Lett.*, *83*(15), 3054, doi:10.1063/1.1617373.

Duputel, Z., V. Ferrazzini, F. Brenguier, N. Shapiro, C. M.,. A. Nercessian, M. Campillo, and A. Nercessian (2009), Real time monitoring of relative velocity changes using ambient seismic noise at the Piton de la Fournaise volcano (La Réunion) from January 2006 to June 2007, *J. Volcanol. Geotherm. Res.*, *184*(1-2), 164–173, doi:10.1016/j.jvolgeores.2008.11.024.

Grêt, A., R. Snieder, and J. Scales (2006), Time-lapse monitoring of rock properties with coda wave interferometry, *J. Geophys. Res.*, *111*, B03305, doi:10.1029/2004JB003354.

Hadziioannou, C., E. Larose, A. Baig, P. Roux, and M. Campillo (2011), Improving temporal resolution in ambient noise monitoring of seismic wave speed, *J. Geophys. Res.*, *116*, B07304, doi:10.1029/2011JB008200.

Hobiger, M., U. Wegler, K. Shiomi, and H. Nakahara (2012), Coseismic and postseismic elastic wave velocity variations caused by the 2008 Iwate-Miyagi Nairiku earthquake, Japan, *J. Geophys. Res.*, *117*, B09313, doi:10.1029/2012JB009402.

Hobiger, M., U. Wegler, K. Shiomi, and H. Nakahara (2014), Single-station cross-correlation analysis of ambient seismic noise: Application to stations in the surroundings of the 2008 Iwate-Miyagi Nairiku earthquake, *Geophys. J. Int.*, *198*(1), 90–109, doi:10.1093/gji/ggu115.

Larose, E., L. Margerin, A. Derode, B. Van Tiggelen, M. Campillo, N. Shapiro, A. Paul, L. Stehly, M. Tanter, and B. van Tiggelen (2006), Correlation of random wavefields: An interdisciplinary review, *Geophysics*, *71*(4), SI11, doi:10.1190/1.2213356.

Lecocq, T., C. Caudron, and F. Brenguier (2014), MSNoise: a Python package for monitoring seismic velocity changes using ambient seismic noise, *Seismol. Res. Lett.*, *85*(3), 715–726, doi:10.1785/0220130073.

Lengliné, O., Z. Duputel, and V. Ferrazzini (2016), Uncovering the hidden signature of a magmatic recharge at Piton de la Fournaise volcano using small earthquakes, *Geophys. Res. Lett.*, *43*, 4255–4262, doi:10.1002/2016GL068383.

Lobkis, O. I., and R. L. Weaver (2001), On the emergence of the Green's function in the correlations of a diffuse field, *J. Acoust. Soc. Am.*, *110*(6), 3011, doi:10.1121/1.1417528.

Maeda, T., K. Obara, and Y. Yukutake (2010), Seismic velocity decrease and recovery related to earthquake swarms in a geothermal area, *Earth, Planets Space*, *62*(9), 685–691, doi:10.5047/eps.2010.08.006.

Massin, F., V. Ferrazzini, P. Bachèlery, A. Nercessian, Z. Duputel, and T. Staudacher (2011), Structures and evolution of the plumbing system of Piton de la Fournaise volcano inferred from clustering of 2007 eruptive cycle seismicity, *J. Volcanol. Geotherm. Res.*, *202*(1-2), 96–106, doi:10.1016/j.jvolgeores.2011.01.008.

Meteo-France Direction Interrégionale Océan Indien (2014), Bulletin Climatologique Annuel 2014, SAINTE CLOTILDE.

Minato, S., T. Tsuji, S. Ohmi, and T. Matsuoka (2012), Monitoring seismic velocity change caused by the 2011 Tohoku-oki earthquake using ambient noise records, *Geophys. Res. Lett.*, *39*, L09309, doi:10.1029/2012GL051405.

Mordret, A., A. D. Jolly, Z. Duputel, and N. Fournier (2010), Monitoring of phreatic eruptions using Interferometry on Retrieved Cross-Correlation Function from Ambient Seismic Noise: Results from Mt. Ruapehu, New Zealand, *J. Volcanol. Geotherm. Res.*, *191*(1–2), 46–59, doi:10.1016/j.jvolgeores.2010.01.010.

Nakahara, H. (2014), Auto correlation analysis of coda waves from local earthquakes for detecting temporal changes in shallow subsurface structures: The 2011 Tohoku-Oki, Japan earthquake, *Pure Appl. Geophys.*, *172*(2), 213–224, doi:10.1007/s00024-014-0849-0.

Ohmi, S., K. Hirahara, H. Wada, and K. Ito (2008), Temporal variations of crustal structure in the source region of the 2007 Noto Hanto Earthquake, central Japan, with passive image interferometry, *Earth Planets Space*, *60*(10), 1069–1074, doi:10.1186/BF03352871.

Patane, D. (2006), Time-resolved seismic tomography detects magma intrusions at Mount Etna, *Science*, *13*(5788), 821–823, doi:10.1126/science.1127724.
Peltier, A., T. Staudacher, P. Bachèlery, and V. Cayol (2009), Formation of the April 2007 caldera collapse at Piton de La Fournaise volcano: Insights from GPS data, *J. Volcanol. Geotherm. Res.*, *184*(1-2), 152–163, doi:10.1016/j.jvolgeores.2008.09.009.
Peltier, A., F. Beauducel, N. Villeneuve, V. Ferrazzini, A. Di Muro, A. Aiuppa, A. Derrien, K. Jourde, and B. Taisne (2016), Deep fluid transfer evidenced by surface deformation during the 2014–2015 unrest at Piton de la Fournaise volcano, *J. Volcanol. Geotherm. Res.*, *321*, 140–148, doi:10.1016/j.jvolgeores.2016.04.031.
Poupinet, G., W. L. Ellsworth, and J. Frechet (1984), Monitoring velocity variations in the crust using earthquake doublets: An application to the Calaveras Fault, California, *J. Geophys. Res.*, *89*, 5719, doi:10.1029/JB089iB07p05719.
Ratdomopurbo, A., and G. Poupinet (1995), Monitoring a temporal change of seismic velocity in a volcano: Application to the 1992 eruption of Mt. Merapi (Indonesia), *Geophys. Res. Lett.*, *22*, 775–778, doi:10.1029/95GL00302.
Rivet, D., F. Brenguier, D. Clarke, N. M. Shapiro, and A. Peltier (2014), Long-term dynamics of Piton de la Fournaise volcano from 13 years of seismic velocity change measurements and GPS observations, *J. Geophys. Res. Solid Earth*, *119*, 7654–7666, doi:10.1002/2014JB011307.
Rivet, D., F. Brenguier, and F. Cappa (2015), Improved detection of preeruptive seismic velocity drops at the Piton de La Fournaise volcano, *Geophys. Res. Lett.*, *42*, 6332–6339, doi:10.1002/2015GL064835.
Schimmel, M. (1999), Phase cross-correlations: Design, comparisons, and applications, *Bull. Seismol. Soc. Am.*, *89*(5), 1366–1378.
Schimmel, M., and J. Gallart (2007), Frequency-dependent phase coherence for noise suppression in seismic array data, *J. Geophys. Res.*, *112*, B04303, doi:10.1029/2006JB004680.
Schimmel, M., E. Stutzmann, and J. Gallart (2011), Using instantaneous phase coherence for signal extraction from ambient noise data at a local to a global scale, *Geophys. J. Int.*, *184*(1), 494–506, doi:10.1111/j.1365-246X.2010.04861.x.
Sens-Schönfelder, C., and U. Wegler (2006), Passive image interferemetry and seasonal variations of seismic velocities at Merapi Volcano, Indonesia, *Geophys. Res. Lett.*, *33*, L21302, doi:10.1029/2006GL027797.
Sens-Schönfelder, C., and U. Wegler (2011), Passive image interferometry for monitoring crustal changes with ambient seismic noise, *Comptes Rendus Geosci.*, *343*(8-9), 639–651, doi:10.1016/j.crte.2011.02.005.
Sens-Schönfelder, C., E. Pomponi, and A. Peltier (2014), Dynamics of Piton de la Fournaise volcano observed by passive image interferometry with multiple references, *J. Volcanol. Geotherm. Res.*, *276*, 32–45, doi:10.1016/j.jvolgeores.2014.02.012.
Snieder, R. (2004), Extracting the Green's function from the correlation of coda waves: A derivation based on stationary phase, *Phys. Rev. E*, *69*(4), doi:10.1103/PhysRevE.69.046610.
Snieder, R., and M. Hagerty (2004), Monitoring change in volcanic interiors using coda wave interferometry: Application to Arenal Volcano, Costa Rica, *Geophys. Res. Lett.*, *31*, L09608, doi:10.1029/2004GL019670.
Staudacher, T., V. Ferrazzini, A. Peltier, P. Kowalski, P. Boissier, P. Catherine, F. Lauret, and F. Massin (2009), The April 2007 eruption and the Dolomieu crater collapse, two major events at Piton de la Fournaise (La Réunion Island, Indian Ocean), *J. Volcanol. Geotherm. Res.*, *184*(1-2), 126–137, doi:10.1016/j.jvolgeores.2008.11.005.
Wapenaar, K. (2004), Retrieving the elastodynamic Green's function of an arbitrary inhomogeneous medium by cross correlation, *Phys. Rev. Lett.*, *93*(25), 1–4, doi:10.1103/PhysRevLett.93.254301.
Wapenaar, K., D. Draganov, R. Snieder, X. Campman, and A. Verdel (2010a), Tutorial on seismic interferometry: Part 1—Basic principles and applications, *Geophysics*, *75*(5), 75A195, doi:10.1190/1.3457445.
Wapenaar, K., E. Slob, R. Snieder, and A. Curtis (2010b), Tutorial on seismic interferometry: Part 2—Underlying theory and new advances, *Geophysics*, *75*(5), 75A211, doi:10.1190/1.3463440.
Wegler, U., and C. Sens-Schönfelder (2007), Fault zone monitoring with passive image interferometry, *Geophys. J. Int.*, *168*(3), 1029–1033, doi:10.1111/j.1365-246X.2006.03284.x.
Wegler, U., H. Nakahara, C. Sens-Schönfelder, M. Korn, and K. Shiomi (2009), Sudden drop of seismic velocity after the 2004 M_w 6.6 mid-Niigata earthquake, Japan, observed with Passive Image Interferometry, *J. Geophys. Res.*, *114*, B06305, doi:10.1029/2008JB005869.
Withers, M. M., R. C. Aster, C. J. Young, and E. P. Chael (1996), High-frequency analysis of seismic background noise as a function of wind speed and shallow depth, *Bull. Seismol. Soc. Am.*, *86*(5), 1507–1515.